

## Investigation of Exchange Bias in Iron Oxide Nanoparticles Based Multilayered Structure

Saira Riaz<sup>1)</sup>, Shahzad Naseem<sup>2)</sup> and \*Usaman Khan

<sup>1), 2)</sup> *Centre of Excellence in Solid State Physics, University of the Punjab, Lahore-54590, Pakistan*

<sup>1)</sup> [saira\\_cssp@yahoo.com](mailto:saira_cssp@yahoo.com)

One of the least explored approaches for new functionalities of spintronic devices is based on direct manipulation of interlayer exchange coupling. In interlayer exchange coupling, the spin in the ferromagnetic layer injects spin polarized electrons to the non-magnetic layer. These electrons then interact with the spins of bottom ferromagnetic electrode that is pinned using an antiferromagnetic layer. This layered structure results in magnetic behavior with the presence of wasp-waist. Such behavior is observed in the present work (i.e. M-H plots) where iron oxide nanoparticles have been synthesized using sol-gel method. Solution temperature is varied as 20-50°C. Diffraction peaks corresponding to (104), (110), (113), (024) and (116) planes confirm the formation of Fe<sub>2</sub>O<sub>3</sub> phase. Crystallite size, crystallinity and saturation magnetization (M<sub>s</sub>) of Fe<sub>2</sub>O<sub>3</sub> NPs increase as the reaction temperature is increased to 40°C. Dielectric constant increases and tangent loss decreases as the reaction temperature is increased to 40°C. Further increase in reaction temperature results in decreased dielectric constant.

### 1. INTRODUCTION

Magnetic iron oxide nanoparticles have been utilized in a range of applications including gas sensors, catalyst, biomedical applications, spintronic and magnetic storage devices (Zhou et al. 2012). Iron oxide exists in several phases including wustite (FeO), magnetite (Fe<sub>3</sub>O<sub>4</sub>), Fe<sub>2</sub>O<sub>3</sub> ( $\alpha$ -Fe<sub>2</sub>O<sub>3</sub>,  $\beta$ -Fe<sub>2</sub>O<sub>3</sub>,  $\gamma$ -Fe<sub>2</sub>O<sub>3</sub>,  $\epsilon$ -Fe<sub>2</sub>O<sub>3</sub>). Out of these phases hematite ( $\alpha$ -Fe<sub>2</sub>O<sub>3</sub>) is of technological importance due to its high chemical and thermal stability (Singh et al. 2013, Ahn et al. 2015, Riaz et al. 2013).

Hematite is also known as ferroic oxide. It is the most stable form of iron oxide as magnetite and maghemite both transform to hematite phase at elevated temperatures. Hematite has band gap of 2.2eV with semiconducting properties. The two conventions used to describe the crystal structure of hematite are: 1) Hexagonal corundum structure, in this case the unit cell is composed of six formula units; 2) Rhombohedral structure: In this case the unit cell has two formula units. Oxygen anions in hematite lattice are arranged in closed pack array along (001) plane (Riaz et al. 2014a,b, Akbar et al. 2014a,b).

---

<sup>1)</sup> Professor

Hematite has weak ferromagnetic behavior. This type of magnetization is associated with presence of canted spins. An important transition in hematite is known as Morin Transition. This transition is associated with changes in magnetic properties from weak magnetic behavior to antiferromagnetic nature. Below Morin temperature the easy axis of magnetization is in the direction of c-axis. At 683°C, hematite exhibits paramagnetic behavior (Levinson 1971, Craik 1975, Ubale et al. 2015).

Different techniques have been used for preparation of iron oxide such as: 1) Solid phase method that includes calcination, auto combustion synthesis etc; 2) Liquid phase synthesis including sol-gel, co-precipitation method, sonolysis, hydrothermal method etc. 3) Gas phase synthesis including laser pyrolysis, chemical vapor deposition. Not only the principle of all of these methods is different but their cost and practicality are also different (Singh et al. 2013).

For synthesis of iron oxide nanoparticles using low cost and application oriented technique sol-gel method was chosen. We here report sol-gel preparation of iron oxide nanoparticles with variation in solution temperature as 30°C, 40°C and 50°C. Effect of solution temperature on various properties was examined.

## **2. EXPERIMENTAL DETAILS**

For synthesis of iron oxide nanoparticles, the precursor used was  $\text{Fe}(\text{NO}_3)_3 \cdot 9\text{H}_2\text{O}$ . Solvent employed in this study was ethylene glycol.  $\text{Fe}(\text{NO}_3)_3 \cdot 9\text{H}_2\text{O}$  was mixed in the solvent. The solution was stirred on hot plate to obtain iron oxide sol and nanoparticles. Solution temperature during sol-gel synthesis was varied as 30°C, 40°C and 50°C. Detailed sol-gel synthesis has been reported elsewhere (Riaz et al. 2014b, Akbar et al. 2014b).

For structural characterization Bruker D8 Advance X-ray diffractometer was used. Magnetic properties were checked using Lakeshore's 7407 Vibrating Sample Magnetometer. Dielectric properties were investigated using 6500B Precision Impedance Analyzer.

## **3. RESULTS AND DISCUSSION**

X-ray diffraction patterns for iron oxide nanoparticles synthesized at solution temperature 30°C, 40°C and 50°C can be seen in Fig. 1. Diffraction peaks are indexed using JCPDS card no. 87-1165. All the diffraction peaks are matched with  $\text{Fe}_2\text{O}_3$  phase of iron oxide. Crystallinity of nanoparticles increases with increase in solution temperature to 40°C. A temperature gradient is established in the sol as solution temperature increases. This temperature gradient is localized around the colloidal particles. As a result of which, mobility of the ions in the solution increases. This results in better bonding capability as compared to nanoparticles prepared at low solution temperature thus increasing the crystallinity of nanoparticles (Azam et al. 2015, Riaz et al. 2015).

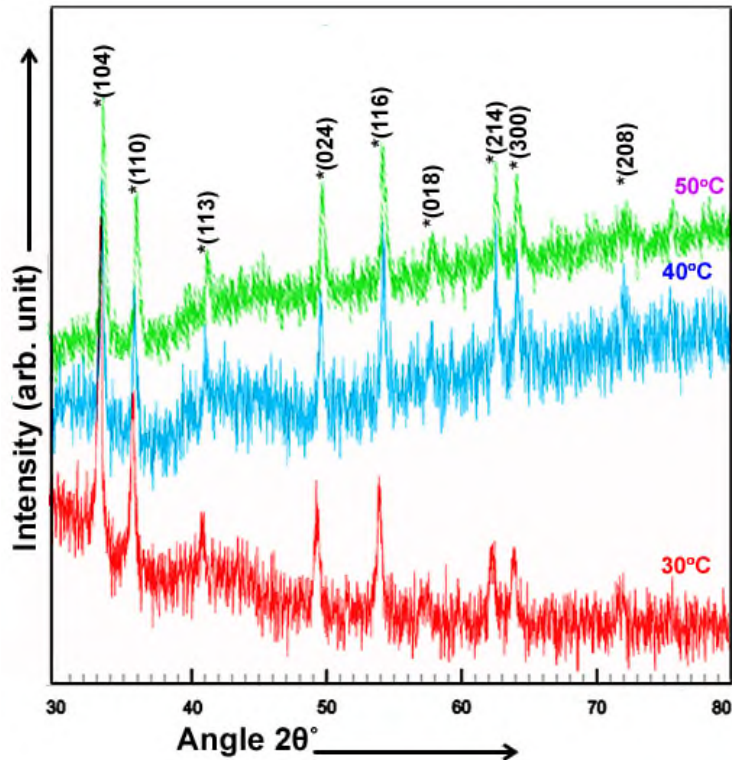


Fig. 1 XRD patterns for iron oxide nanoparticles prepared with variation in solution temperature

Crystallite size ( $t$ ) (Cullity 1956), dislocation density ( $\delta$ ) (Kumar et al. 2011) and lattice parameters (Cullity 1956) were calculated using Eqs. 1-3

$$t = \frac{0.9\lambda}{B \cos \theta} \quad (1)$$

$$\delta = \frac{1}{t^2} \quad (2)$$

$$\sin^2 \theta = \frac{\lambda^2}{3a^2} (h^2 + k^2 + hk) + \frac{\lambda^2 l^2}{4c^2} \quad (3)$$

Where,  $\theta$  is the diffraction angle,  $\lambda$  is the wavelength (1.5406Å) and  $B$  is Full Width at Half Maximum. Increase in crystallite size (table 1) takes place with increase in solution temperature to 40°C resulting in decrease in dislocation density. As solution temperature increased to 50°C decrease in crystallite size was observed with increase in dislocation density. As reaction temperature of solution increased there is a localized heating around the ions. This leads to temperature gradient in the sol. This temperature gradient is responsible for impediment of Ostwald ripening mechanism at high reaction temperatures thus resulting in decrease in crystallite size (Riaz et al. 2015, Azam et al. 2015). Lattice parameters for iron oxide nanoparticles are close to those reported in the literature (Riaz et al. 2014a, Akbar et al. 2014b).

Table 1 Structural parameters for iron oxide nanoparticles

Solution temperature (°C)	Crystallite size (nm)	Dislocation density ( $10^{15}$ lines/m <sup>2</sup> )	Lattice parameters (Å)		Unit cell volume
			a	C	
30	23.45	1.818504	5.014	13.532	294.6107
40	25.64	1.521122	5.013	13.512	294.058
50	22.14	2.040069	5.095	13.510	303.7118

Dielectric constant ( $\epsilon$ ) and tangent loss ( $\tan \delta$ ) were calculated using Eqs. 4 and 5 (Barsoukov and Macdonald 2005)

$$\epsilon = \frac{Cd}{\epsilon_0 A} \quad (4)$$

$$\tan \delta = \frac{1}{2\pi f \epsilon_0 \epsilon \rho} \quad (5)$$

Where, C is the capacitance,  $\epsilon_0$  is the permittivity of free space, A is the area, f is the frequency and  $\rho$  is the resistivity. Dielectric constant and tangent loss show Debye type dispersion. The Debye type dispersion is associated with Koop's theory. In accordance with this theory, grains are active at high frequencies and grain boundaries are active at low frequencies. In case of nanoparticles when grain sizes are reduced number of grain boundaries increases. As the size is reduced dielectric constant is reduced due to the presence of large number of grain boundaries (Riaz et al. 2015, Azam et al. 2015, Barsoukov and Macdonald 2005). Dielectric constant (Fig. 2(a)) increases with increase in solution temperature to 40°C. This increase in dielectric constant is associated with increased crystallinity of iron oxide nanoparticles and decrease in dislocation density as was observed in Fig. 1 and table 1. It is important mentioning here that dielectric constant of iron oxide nanoparticles prepared with variation in solution temperature are high as compared to that reported in literature (Iwachi 1971, Mirza et al. 2015)

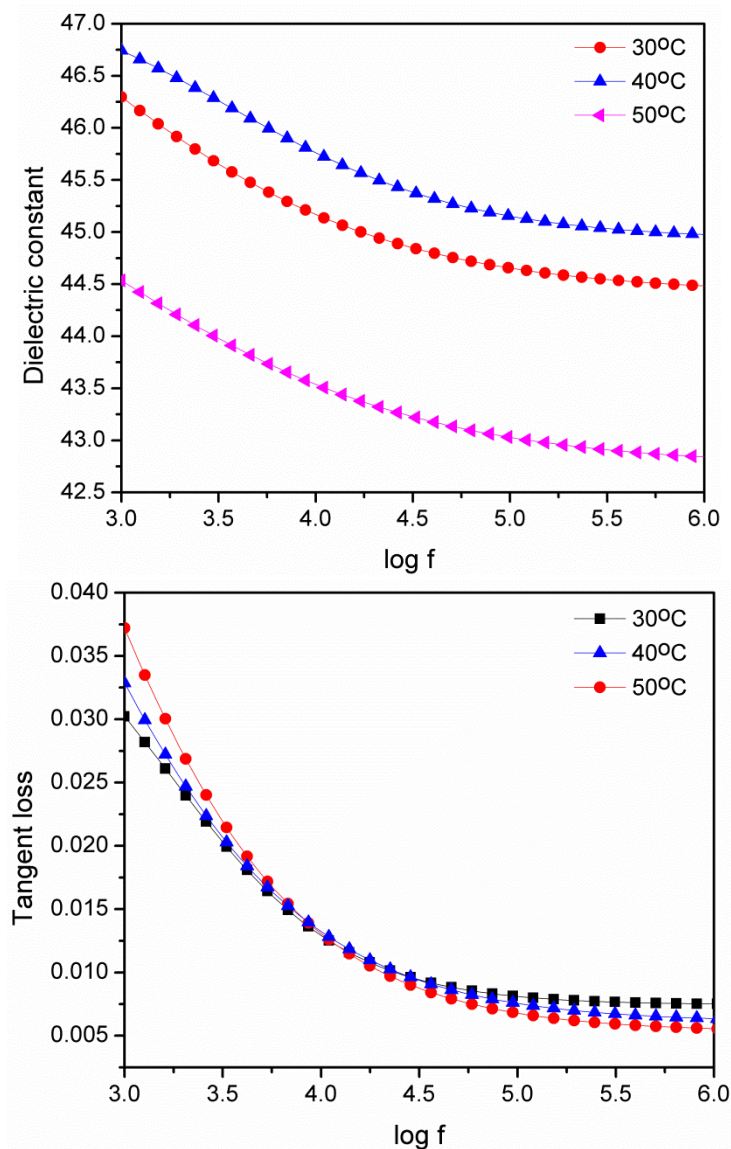


Fig. 2 Dielectric constant and tangent loss for iron oxide nanoparticles

Magnetic hysteresis curves (Fig. 3) for iron oxide nanoparticles synthesized using solution temperature 40°C results in M-H loop equivalent to layered structure. One of the least discovered approaches for spintronic devices is based on direct exploitation of interlayer exchange coupling. In interlayer exchange coupling, ferromagnetic layer inject spin polarized electrons to the non-magnetic layer. Due to delocalization of conduction electrons, the polarized electrons will travel through the non-magnetic layer. These electrons then interact with the spins of bottom ferromagnetic electrode that is pinned by using an antiferromagnetic layer (Ziese and Thornton 2001). This layered structure results in magnetic behavior with the presence of wasp-waist. However, it can be seen that such behavior has been observed in nanoparticles (Fig. 3) indicating that the layered structure like behavior used in spintronic devices has been achieved. It is important mentioning here that such magnetic behavior has been previously reported

using either multilayers (Ziese and Thornton 2001) or with doping of various materials in single phase materials (Ashraf et al. 2014). But such magnetic behavior in single phase iron oxide nanoparticles has never been reported earlier.

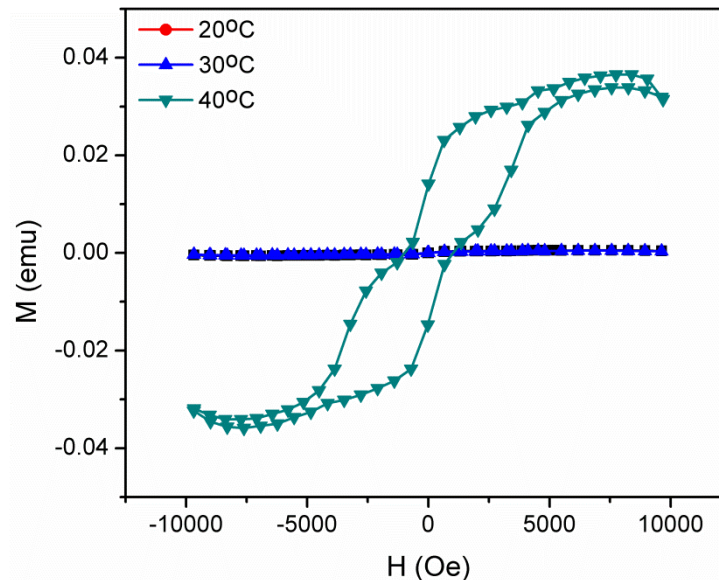


Fig. 3 M-H curves for iron oxide nanoparticles

#### 4. CONCLUSIONS

Fe<sub>2</sub>O<sub>3</sub> nanoparticles were synthesized via sol-gel process with variation in solution temperature as 30°C, 40°C and 50°C. Phase formation of Fe<sub>2</sub>O<sub>3</sub> was confirmed using X-ray diffraction patterns. Crystallinity and dielectric constant of nanoparticles increased with increase in solution temperature to 40°C. Iron oxide nanoparticles prepared at solution temperature 40°C resulted in M-H curve equivalent to layered structure used in spintronic devices.

#### REFERENCES

- Ahn, C.W., Choi, J.J., Ryu, J., Hahn, B.D., Kim, J.W., Yoon, W.H., Choi, J.H. and Park, D.S. (2015), "Microstructure and electrochemical properties of iron oxide film fabricated by aerosol deposition method for lithium ion battery," *Journal of Pow. Sour.*, **275**, 336-340.
- Akbar, A., Riaz, S., Ashraf, R. and Naseem, S. (2014(b)), "Magnetic and magnetization properties of Co-doped Fe<sub>2</sub>O<sub>3</sub> thin films," *IEEE Trans. Magn.*, **50**, 2201204
- Akbar, A., Riaz, S., Bashir, M. and Naseem, S. (2014a), "Effect of Fe<sup>3+</sup>/Fe<sup>2+</sup> Ratio on Superparamagnetic Behavior of Spin Coated Iron Oxide Thin Films," *IEE Trans. Magn.*, **50**, 2200804.

- Ashraf, R., Riaz, S., Bashir, M., Khan, U. and Naseem, S. (2014), "Structural and Magnetic Properties of Mn/Fe Co-Doped ZnO Thin Films Prepared by Sol-Gel Technique," *IEEE Trans. Magn.*, **50**, 2401204
- Azam. M., Riaz, S., Akbar, A. and Naseem, S. (2015), "Structural, magnetic and dielectric properties of spinel  $MgFe_2O_4$  by sol-gel route," *J. Sol-Gel Sci. Technol.*, **74**, 340–351.
- Barsoukov, E. and Macdonald, J.R. (2005), "Impedance Spectroscopy Theory, Experiment, and Applications," John Wiley & Sons, Inc., Publication, New Jersey, 2005.
- Cadappa, D.C., Sanjayan, J.G. and Setunge, S. (2001), "Complete triaxial stress-strain curves of high-strength concrete," *J. Mat. Civil Eng., ASCE*, **13**(3), 209-215.
- Chern, J.C., Yang, H.J. and Chen, H.W. (1992), "Behavior of steel fiber reinforced concrete in multi axial loading", *ACI Mat. J.*, **89**(1), 32-40.
- Cullity, B.D. (1956), "Elements of x-ray diffraction," Addison Wesley Publishing Company, USA.
- Kumar, N., Sharma, V., Parihar, U., Sachdeva, R., Padha, N. and Panchal, C.J. (2011) "Structure, optical and electrical characterization of tin selenide thin films deposited at room temperature using thermal evaporation method," *J. Nano- Electron. Phys.*, **3**, 117-126
- Levinson, L.M. (1971), "Temperature Dependence of the Weak Ferromagnetic Moment of Hematite," *Phys. Rev. B*, **3**, 1971
- Mirza, I., Ali, K., Sarfraz, A.K., Ali, A. and Haq, A. (2015), "A study of dielectric, optical and magnetic characteristics of maghemite nanocrystallites," *Mater. Chem. Phys.*, **164**, 183-187
- Riaz, S., Akbar, A. and Naseem, S. (2013), "Structural, electrical and magnetic properties of iron oxide thin films," *Adv. Sci. Lett.*, **19**, 828-833.
- Riaz, S., Akbar, A. and Naseem, S. (2014a), "Ferromagnetic Effects in Cr-Doped  $Fe_2O_3$  Thin Films," *IEEE Trans. Magn.*, **50**, 2200704
- Riaz, S., Ashraf, R., Akbar, A. and Naseem, S. (2014b), "Free Growth of Iron Oxide Nanostructures by Sol-Gel Spin Coating Technique—Structural and Magnetic Properties," *IEE Trans. Magn.*, **50**, 2301805.
- Riaz, S., Shah, S.M.H., Akbar, A., Atiq, S., Naseem, S. (2015), "Effect of Mn doping on structural, dielectric and magnetic properties of  $BiFeO_3$  thin films," *J. Sol-Gel Sci. Technol.*, **74**, 329-339
- Singh, M., Ulbrich, P., Prokopec, V., Svoboda, P., Santava, E. and Stepanek, F. (2013), "Vapour phase approach for iron oxide nanoparticle synthesis from solid precursors," *J. Solid State Chem.*, **200**, 150–156
- Ubale, A.U. and Belkhedkar. M.R. (2015), "Size Dependent Physical Properties of Nanostructured  $\alpha-Fe_2O_3$  Thin Films Grown by Successive Ionic Layer Adsorption and reaction Method for Antibacterial Application," *J. Mater. Sci. Technol.*, **31**(1), 1-9.
- Zhou, X., Shi, Y., Ren, L., Bao, S., Han, Y., Wu, S., Zhang, H., Zhong, L. and Zhang, Q. (2012), "Controllable synthesis, magnetic and biocompatible properties of  $Fe_3O_4$  and  $\alpha-Fe_2O_3$  nanocrystals," *J. Solid State Chem.*, **196**, 138–144
- Ziese, M. and Thornton, M.J. (2001), Spin Electronics, Springer-Verlag, Berlin